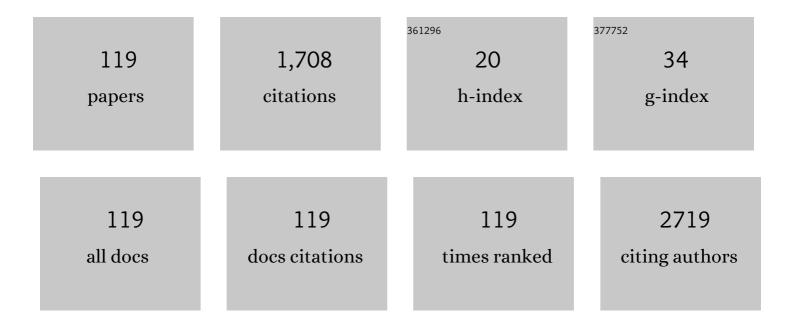
Mann-Ho Cho

List of Publications by Year in descending order

Source: https://exaly.com/author-pdf/5086894/publications.pdf Version: 2024-02-01



#	Article	IF	CITATIONS
1	Enhancement in thermoelectric properties of Te-embedded Bi2Te3 by preferential phonon scattering in heterostructure interface. Nano Energy, 2018, 47, 374-384.	8.2	101
2	MoS ₂ –InGaZnO Heterojunction Phototransistors with Broad Spectral Responsivity. ACS Applied Materials & Interfaces, 2016, 8, 8576-8582.	4.0	98
3	Interaction- and defect-free van der Waals contacts between metals and two-dimensional semiconductors. Nature Electronics, 2022, 5, 241-247.	13.1	84
4	Wafer-scale synthesis of thickness-controllable MoS ₂ films via solution-processing using a dimethylformamide/n-butylamine/2-aminoethanol solvent system. Nanoscale, 2015, 7, 9311-9319.	2.8	82
5	Terahertz single conductance quantum and topological phase transitions in topological insulator Bi2Se3 ultrathin films. Nature Communications, 2015, 6, 6552.	5.8	79
6	High concentration of nitrogen doped into graphene using N ₂ plasma with an aluminum oxide buffer layer. Journal of Materials Chemistry C, 2014, 2, 933-939.	2.7	62
7	Improved thermal stability of Al2O3/HfO2/Al2O3 high-k gate dielectric stack on GaAs. Applied Physics Letters, 2010, 96, .	1.5	55
8	The electronic structure of C60/ZnPc interface for organic photovoltaic device with blended layer architecture. Applied Physics Letters, 2010, 96, .	1.5	50
9	Thermal and Electrical Conduction of Single-crystal Bi2Te3 Nanostructures grown using a one step process. Scientific Reports, 2016, 6, 19132.	1.6	45
10	Structural Evolution and the Control of Defects in Atomic Layer Deposited HfO ₂ –Al ₂ O ₃ Stacked Films on GaAs. ACS Applied Materials & Interfaces, 2013, 5, 1982-1989.	4.0	34
11	Evolution of crystal structures in GeTe during phase transition. Scientific Reports, 2017, 7, 955.	1.6	32
12	Non-toxically enhanced sulfur reaction for formation of chalcogenide thin films using a thermal cracker. Journal of Materials Chemistry A, 2014, 2, 14593-14599.	5.2	31
13	Reversible Fermi Level Tuning of a Sb ₂ Te ₃ Topological Insulator by Structural Deformation. Nano Letters, 2015, 15, 3820-3826.	4.5	31
14	Controlling the defects and transition layer in SiO2 films grown on 4H-SiC via direct plasma-assisted oxidation. Scientific Reports, 2016, 6, 34945.	1.6	29
15	Effect of the Thermal Conductivity on Resistive Switching in GeTe and Ge ₂ Sb ₂ Te ₅ Nanowires. ACS Applied Materials & Interfaces, 2015, 7, 21819-21827.	4.0	25
16	Tuning the Fermi level with topological phase transition by internal strain in a topological insulator Bi ₂ Se ₃ thin film. Nanoscale, 2016, 8, 741-751.	2.8	23
17	P–N Junction Diode Using Plasma Boron-Doped Black Phosphorus for High-Performance Photovoltaic Devices. ACS Nano, 2019, 13, 1683-1693.	7.3	23
18	Al ₂ O ₃ Passivation Effect in HfO ₂ ·Al ₂ O ₃ Laminate Structures Grown on InP Substrates. ACS Applied Materials & Interfaces, 2017, 9, 17526-17535.	4.0	22

Μανν-Ηο Cho

#	Article	IF	CITATIONS
19	Ultrafast phase change and long durability of BN-incorporated GeSbTe. Journal of Materials Chemistry C, 2015, 3, 1707-1715.	2.7	21
20	The effect of ZnO surface conditions on the electronic structure of the ZnO/CuPc interface. Applied Physics Letters, 2011, 98, 082111.	1.5	20
21	Modulation of phase change characteristics in Ag-incorporated Ge ₂ Sb ₂ Te ₅ owing to changes in structural distortion and bond strength. Journal of Materials Chemistry C, 2017, 5, 3973-3982.	2.7	20
22	Closing the Surface Bandgap in Thin Bi ₂ Se ₃ /Graphene Heterostructures. ACS Nano, 2019, 13, 3931-3939.	7.3	20
23	Effect of In incorporated into SbTe on phase change characteristics resulting from changes in electronic structure. Applied Physics Letters, 2010, 96, 052112.	1.5	19
24	Na-Dependent Ultrafast Carrier Dynamics of CdS/Cu(In,Ga)Se2 Measured by Optical Pump-Terahertz Probe Spectroscopy. Journal of Physical Chemistry C, 2015, 119, 20231-20236.	1.5	19
25	Filament Geometry Induced Bipolar, Complementary and Unipolar Resistive Switching under the Same Set Current Compliance in Pt/SiOx/TiN. Scientific Reports, 2015, 5, 15374.	1.6	18
26	Electric field effect dominated bipolar resistive switching through interface control in a Pt/TiO ₂ /TiN structure. RSC Advances, 2015, 5, 221-230.	1.7	18
27	Structural and Electrical Properties of EOT HfO ₂ (<1 nm) Grown on InAs by Atomic Layer Deposition and Its Thermal Stability. ACS Applied Materials & Interfaces, 2016, 8, 7489-7498.	4.0	18
28	Ultra-low Energy Phase Change Memory with Improved Thermal Stability by Tailoring the Local Structure through Ag Doping. ACS Applied Materials & Interfaces, 2020, 12, 37285-37294.	4.0	18
29	Electrical properties and thermal stability in stack structure of HfO2/Al2O3/InSb by atomic layer deposition. Scientific Reports, 2017, 7, 11337.	1.6	17
30	Characterization of Rotational Stacking Layers in Large-Area MoSe ₂ Film Grown by Molecular Beam Epitaxy and Interaction with Photon. ACS Applied Materials & Interfaces, 2017, 9, 30786-30796.	4.0	16
31	Effects of Nitrogen Incorporation in HfO ₂ Grown on InP by Atomic Layer Deposition: An Evolution in Structural, Chemical, and Electrical Characteristics. ACS Applied Materials & Map; Interfaces, 2014, 6, 3896-3906.	4.0	15
32	Enhancement of carrier lifetime by spin–orbit coupling in a topological insulator of an Sb ₂ Te ₃ thin film. Nanoscale, 2016, 8, 19025-19035.	2.8	15
33	Phase Transformation of Alternately Layered Bi/Se Structures to Well-Ordered Single Crystalline Bi ₂ Se ₃ Structures by a Self-Organized Ordering Process. Journal of Physical Chemistry C, 2012, 116, 3737-3746.	1.5	14
34	The effect of copper hexadecafluorophthalocyanine (F16CuPc) inter-layer on pentacene thin-film transistors. Synthetic Metals, 2010, 160, 108-112.	2.1	13
35	Phase Transformation through Metastable Structures in Atomically Controlled Se/Sb MultiLayers. Journal of Physical Chemistry C, 2011, 115, 13462-13470.	1.5	13
36	Effect of amorphization on the structural stability and reversibility of Ge2Sb2Te5 and oxygen incorporated Ge2Sb2Te5 films. Journal of Materials Chemistry, 2012, 22, 16527.	6.7	13

#	Article	IF	CITATIONS
37	Ultrafast photocarrier dynamics related to defect states of Si _{1â^'x} Ge _x nanowires measured by optical pump–THz probe spectroscopy. Nanoscale, 2017, 9, 8015-8023.	2.8	13
38	Evolution of the broadband optical transition in large-area <mml:math xmlns:mml="http://www.w3.org/1998/Math/MathML"><mml:mrow><mml:mi>MoS</mml:mi><mml:msub><mml: mathvariant="normal">e<mml:mn>2</mml:mn></mml: </mml:msub></mml:mrow>. Physical Review B, 2018, 97, .</mml:math 	mi 1.1	13
39	Improving Electrical Properties by Effective Sulfur Passivation via Modifying the Surface State of Substrate in HfO ₂ /InP Systems. Journal of Physical Chemistry C, 2018, 122, 7226-7235.	1.5	13
40	The Phase Change Effect of Oxygen-Incorporation in GeSbTe Films. Journal of the Electrochemical Society, 2011, 158, H471.	1.3	12
41	Effects of Interface Al[sub 2]O[sub 3] Passivation Layer for High-k HfO[sub 2] on GaAs. Electrochemical and Solid-State Letters, 2011, 14, H63.	2.2	12
42	Evolution of the surface state in Bi ₂ Se ₂ Te thin films during phase transition. Nanoscale, 2015, 7, 14924-14936.	2.8	12
43	Laser irradiation-induced modification of the amorphous phase in GeTe films: the role of intermediate Ge–Te bonding in the crystallization mechanism. Journal of Materials Chemistry C, 2015, 3, 9393-9402.	2.7	12
44	Enhanced Photoinduced Carrier Generation Efficiency through Surface Band Bending in Topological Insulator Bi ₂ Se ₃ Thin Films by the Oxidized Layer. ACS Applied Materials & Interfaces, 2020, 12, 26649-26658.	4.0	12
45	Effects of hydrogen on Au migration and the growth kinetics of Si nanowires. CrystEngComm, 2011, 13, 690-696.	1.3	11
46	Ultrafast chemical lithiation of single crystalline silicon nanowires: in situ characterization and first principles modeling. RSC Advances, 2015, 5, 17438-17443.	1.7	11
47	Electronic Structure of C60/Zinc Phthalocyanine/V2O5 Interfaces Studied Using Photoemission Spectroscopy for Organic Photovoltaic Applications. Molecules, 2018, 23, 449.	1.7	11
48	Growth of pure wurtzite InGaAs nanowires for photovoltaic and energy harvesting applications. Nano Energy, 2018, 53, 57-65.	8.2	11
49	Ultrafast Photoâ€Response by Surface Stateâ€Mediated Optical Transitions in Topological Insulator Bi ₂ Te ₃ Nanowire. Advanced Optical Materials, 2019, 7, 1900621.	3.6	11
50	Enhanced Spin-to-Charge Conversion Efficiency in Ultrathin Bi ₂ Se ₃ Observed by Spintronic Terahertz Spectroscopy. ACS Applied Materials & Interfaces, 2021, 13, 23153-23160.	4.0	11
51	Improvement of electrical performance using PtSe2/PtTe2 edge contact synthesized by molecular beam epitaxy. Applied Surface Science, 2022, 585, 152507.	3.1	11
52	Thermal Stability of ALD-HfO ₂ /GaAs Pretreated with Trimethylaluminium. Journal of the Electrochemical Society, 2011, 159, G6-G10.	1.3	10
53	Modulation of optoelectronic properties of the Bi2Te3 nanowire by controlling the formation of selective surface oxidation. Applied Surface Science, 2021, 548, 149069.	3.1	10
54	Ferroelastic–Ferroelectric Multiferroicity in van der Waals Rhenium Dichalcogenides. Advanced Materials, 2022, 34, e2108777.	11.1	10

Μανν-Ηο Cho

#	Article	IF	CITATIONS
55	Electronic Structure of Te/Sb/Ge and Sb/Te/Ge Multi Layer Films Using Photoelectron Spectroscopy. Journal of the American Chemical Society, 2009, 131, 13634-13638.	6.6	9
56	The modulation of Si1â^'xGex nanowires by correlation of inlet gas ratio with H2 gas content. CrystEngComm, 2011, 13, 5204.	1.3	9
57	Anomalous Stagewise Lithiation of Gold-Coated Silicon Nanowires: A Combined In Situ Characterization and First-Principles Study. ACS Applied Materials & Interfaces, 2015, 7, 16976-16983.	4.0	9
58	Tuning of Topological Dirac States via Modification of van der Waals Gap in Strained Ultrathin Bi ₂ Se ₃ Films. Journal of Physical Chemistry C, 2018, 122, 23739-23748.	1.5	9
59	Disorder-induced decoupled surface transport channels in thin films of doped topological insulators. Physical Review B, 2018, 98, .	1.1	9
60	Trap-assisted high responsivity of a phototransistor using bi-layer MoSe2 grown by molecular beam epitaxy. Applied Surface Science, 2019, 494, 37-45.	3.1	9
61	Effects of oxygen incorporation in GeSbTe films on electrical properties and thermal stability. Applied Physics Letters, 2010, 96, .	1.5	8
62	Hall mobility manipulation in TiO2â^'x semiconductor films by hydrogen-ion irradiation. Journal of the Korean Physical Society, 2013, 62, 781-786.	0.3	8
63	Defect States below the Conduction Band Edge of HfO2 Grown on InP by Atomic Layer Deposition. Journal of Physical Chemistry C, 2015, 119, 6001-6008.	1.5	8
64	Surface chemical structure and doping characteristics of boron-doped Si nanowires fabricated by plasma doping. Applied Surface Science, 2017, 419, 1-8.	3.1	8
65	Effects of thermal and electrical stress on defect generation in InAs metal–oxide–semiconductor capacitor. Applied Surface Science, 2019, 467-468, 1161-1169.	3.1	8
66	Enhancement of photoresponse in Bi2Se3/graphene heterostructures by effective electron–hole separation through internal band bending. Applied Surface Science, 2021, 554, 149623.	3.1	8
67	Topological Surfaceâ€Đominated Spintronic THz Emission in Topologically Nontrivial Bi _{1â^'} <i>_x</i> Sb <i>_x</i> Films. Advanced Science, 2022, 9, .	5.6	8
68	Relaxation of misfit strain in silicon-germanium (Si1â^'xGex) films during dry oxidation. Journal of Vacuum Science and Technology B:Nanotechnology and Microelectronics, 2010, 28, 1298-1303.	0.6	7
69	The origin of the resistance change in GeSbTe films. Applied Physics Letters, 2010, 97, 152113.	1.5	7
70	Synthesis of self-ordered Sb2Te2 films with atomically aligned Te layers and the effect of phonon scattering modulation. Journal of Materials Chemistry C, 2013, 1, 7043.	2.7	7
71	Effects of spontaneous nitrogen incorporation by a 4H-SiC(0001) surface caused by plasma nitridation. Journal of Materials Chemistry C, 2015, 3, 5078-5088.	2.7	7
72	Effects of resonant bonding and structural distortion on the phase change properties of Sn ₂ Sb ₂ Se ₅ . Journal of Materials Chemistry C, 2017, 5, 7820-7829.	2.7	7

#	Article	IF	CITATIONS
73	Ferroelectric switching in GeTe through rotation of lone-pair electrons by Electric field-driven phase transition. Applied Materials Today, 2021, 24, 101122.	2.3	7
74	Ultrathin platinum diselenide synthesis controlling initial growth kinetics: Interfacial reaction depending on thickness and substrate. Applied Surface Science, 2021, 564, 150300.	3.1	7
75	GeTe Nanosheets as Theranostic Agents for Multimodal Imaging and Therapy of Inflammatory Bowel Disease. Advanced Functional Materials, 2022, 32, 2107433.	7.8	7
76	Thermal instability of HfO ₂ on InP structure with ultrathin Al ₂ O ₃ interface passivation layer. Physica Status Solidi - Rapid Research Letters, 2012, 6, 247-249.	1.2	6
77	The oxidation characteristics of silicon nanowires grown with an au catalyst. Nano Research, 2012, 5, 152-163.	5.8	6
78	Interface engineering for a stable chemical structure of oxidized-black phosphorus <i>via</i> self-reduction in AlO _x atomic layer deposition. Nanoscale, 2018, 10, 22896-22907.	2.8	6
79	Effect of substrate on photo-induced persistent photoconductivity in InAs nanowires. Applied Surface Science, 2018, 458, 964-971.	3.1	6
80	Structural Evolution and Electrical Properties of Highly Active Plasma Process on 4H-SiC. Applied Science and Convergence Technology, 2017, 26, 133-138.	0.3	6
81	Topological insulator bismuth selenide grown on black phosphorus for sensitive broadband photodetection. Journal of Materials Chemistry C, 2021, 9, 15150-15157.	2.7	6
82	Structural deformation and void formation driven by phase transformation in the Ge2Sb2Te5 film. Journal of Materials Chemistry C, 2014, 2, 2001.	2.7	5
83	Structural evolution and carrier scattering of Si nanowires as a function of oxidation time. Journal of Materials Chemistry C, 2015, 3, 2123-2131.	2.7	5
84	Effect of nitrogen incorporation and oxygen vacancy on electronic structure and the absence of a gap state in HfSiO films. Surface Science, 2012, 606, L64-L68.	0.8	4
85	Generation of planar defects caused by the surface diffusion of Au atoms on SiNWs. Materials Research Bulletin, 2012, 47, 2739-2743.	2.7	4
86	High-mobility property of crystallized In-Te chalcogenide materials. Electronic Materials Letters, 2012, 8, 175-178.	1.0	4
87	Electrical characteristics of HfO ₂ films on InP with different atomic-layer-deposition temperatures. Physica Status Solidi (A) Applications and Materials Science, 2013, 210, 1381-1385.	0.8	4
88	Change in crystalline structure and band alignment in atomic-layer-deposited HfO ₂ on InP using an annealing treatment. Physica Status Solidi (A) Applications and Materials Science, 2013, 210, 1612-1617.	0.8	4
89	Phase-change like process through bond switching in distorted and resonantly bonded crystal. Scientific Reports, 2019, 9, 12816.	1.6	4
90	Topological Phase Control of Surface States in Bi2Se3 via Spin–Orbit Coupling Modulation through Interface Engineering between HfO2–X. ACS Applied Materials & Interfaces, 2020, 12, 12215-12226.	4.0	4

#	Article	IF	CITATIONS
91	Enhanced reliability of phase-change memory <i>via</i> modulation of local structure and chemical bonding by incorporating carbon in Ge ₂ Sb ₂ Te ₅ . RSC Advances, 2021, 11, 22479-22488.	1.7	4
92	Improvements in Thermal Stability of Sb ₂ Te ₃ by Modulation of Microstructure via Carbon Incorporation. ACS Applied Electronic Materials, 2021, 3, 3472-3481.	2.0	4
93	The interfacial electronic structure of fullerene/ultra thin dielectrics of SiO2 and SiON. Chemical Physics Letters, 2010, 499, 136-140.	1.2	3
94	A Triple-Layered Microcavity Structure for Electrophoretic Image Display. IEEE Transactions on Electron Devices, 2011, 58, 1116-1120.	1.6	3
95	Induction of the surface plasmon resonance from C-incorporated Au catalyst in Silâ^'xCx nanowires. Journal of Materials Chemistry, 2012, 22, 19744.	6.7	3
96	The effect of structural and chemical bonding changes on the optical properties of Si/Si1â^'xCx core/shell nanowires. Journal of Materials Chemistry C, 2013, 1, 5207.	2.7	3
97	Investigation of silicon-germanium nanowires THz emission. , 2014, , .		3
98	Phase-change-induced martensitic deformation and slip system in GeSbTe. RSC Advances, 2015, 5, 35792-35800.	1.7	3
99	In situ thermal behavior of resistance drift in GeTe and Ge2Sb2Te5 nanowires via Raman thermometry. Journal of Materials Chemistry C, 2020, 8, 11032-11041.	2.7	3
100	Optical characteristics of type-II hexagonal-shaped GaSb quantum dots on GaAs synthesized using nanowire self-growth mechanism from Ga metal droplet. Scientific Reports, 2021, 11, 7699.	1.6	3
101	Ternary Devices Based on Partially Aligned MoS 2 / h â€BN/Graphene Heterostructures. Advanced Materials Interfaces, 2021, 8, 2101109.	1.9	3
102	Control of the interfacial reaction in HfO2 on Si-passivated GaAs. Applied Surface Science, 2013, 283, 375-381.	3.1	2
103	Preparation of Ge-Sb-Te Thin Films by Tellurization of Ge-Sb Thin Film for Phase-Change Random-Access Memory Application. ECS Journal of Solid State Science and Technology, 2019, 8, P298-P302.	0.9	2
104	Quasicrystalline phase-change memory. Scientific Reports, 2020, 10, 13673.	1.6	2
105	Switching to Hidden Metallic Crystal Phase in Phase-Change Materials by Photoenhanced Metavalent Bonding. ACS Nano, 2022, , .	7.3	2
106	Change of resistive-switching in TiO2 films with additional HfO2 thin layer. Journal of the Korean Physical Society, 2012, 60, 1313-1316.	0.3	1
107	Temperature-dependent catalyst-free growth of ZnO nanostructures on Si and SiO2/Si substrates via thermal evaporation. Journal of the Korean Physical Society, 2012, 60, 1877-1885.	0.3	1
108	Phase Change <i>via</i> Intermediary Metastable Local Structure of Ge Atoms in Ge ₂ Sb ₂ Te ₅ Nanowires during Electrical Switching. ACS Applied Electronic Materials, 2020, 2, 2418-2428.	2.0	1

#	Article	IF	CITATIONS
109	Quantification of point and line defects in Si0.6Ge0.4 alloys with thickness variation via optical pump-THz probe measurement. Applied Surface Science, 2020, 513, 145815.	3.1	1
110	Suppression of the Hybridization of Surface States and Transport Property in Ultrathin Bi ₂ Se ₃ /graphene Heterostructure. Applied Science and Convergence Technology, 2019, 28, 207-212.	0.3	1
111	Spatially inhomogeneous operation of phase-change memory. Applied Surface Science, 2022, 589, 153026.	3.1	1
112	The Study of Hafnium Silicate by Various Nitrogen Gas Annealing Treatment. Materials Research Society Symposia Proceedings, 2008, 1073, 1.	0.1	0
113	Interfacial reaction induced strain relaxation in Hf-silicate film on strained Si0.7Ge0.3(001) as a function of annealing temperature. Physica Status Solidi (A) Applications and Materials Science, 2013, 210, 2499-2502.	0.8	0
114	Ultrafast nonequilibrium carrier dynamics of 2D materials measured by time resolved THz spectroscopy. , 2015, , .		0
115	Terahertz spectroscopy of topological insulator Sb <inf>2</inf> Se <inf>3</inf> and its ultrafast nonequilibrium carrier dynamics. , 2016, , .		0
116	Oxidation Mechanism of Sil–xGex Nanowires with Au Catalyst Tip as a Function of Ge Content. ACS Applied Materials & Interfaces, 2017, 9, 37411-37418.	4.0	0
117	Time resolved terahertz spectroscopy of topological insulator Sb <inf>2</inf> Te <inf>3</inf> ., 2017, , .		0
118	Phase-change properties related to anharmonicity of local structure. Current Applied Physics, 2020, 20, 807-816.	1.1	0
119	Controlling the Charge Carrier Density of Black Phosphorus in a Rapid Plasma Doping Process. Applied Science and Convergence Technology, 2020, 29, 176-179.	0.3	О